

Cite this: DOI: 10.1039/c0xx00000x

www.rsc.org/xxxxxx

ARTICLE TYPE

Ultrafast vibrational energy relaxation of the water bridge

Lukasz Piatkowski,^{*a} Adam D. Wexler,^b Elmar C. Fuchs,^b Hinc Schoenmaker^a and Huib J. Bakker^a

Received (in XXX, XXX) Xth XXXXXXXXX 20XX, Accepted Xth XXXXXXXXX 20XX

DOI: 10.1039/b000000x

5 We report the energy relaxation of the OH stretch vibration of HDO molecules contained in an HDO:D₂O water bridge using femtosecond mid-infrared pump-probe spectroscopy. We found that the vibrational lifetime is shorter (~630±50 fs) than for HDO molecules in bulk HDO:D₂O (~740±40 fs). In contrast, the thermalization dynamics following the vibrational relaxation are much slower (~1.5±0.4 ps) than in bulk HDO:D₂O (~250±90 fs). These differences in energy relaxation dynamics strongly indicate that the water
10 bridge and bulk water differ on a molecular scale.

Introduction

The water bridge is an intriguing phenomenon that occurs when a high (~kV/cm) potential difference is applied between two beakers of water. Induced by the field, the water jumps to the
15 edges of the beakers and creates a free hanging string through air connecting the two beakers. In spite of its ease of generation, the physical mechanism behind the formation of the water bridge and its relation to the microscopic properties of water are not completely understood.

20 The discovery of water bridge phenomena goes back to the 19th century, when in 1893 William Armstrong reported his discovery to the public for the first time.¹ Over the next century scientists studied related effects, like electrowetting² or the Sumoto effect³, but the water bridge itself had been forgotten until its recent
25 rediscovery.

The main difficulties in studying the water bridge are its shape and fluctuating width. In addition, the presence of high electric fields and instabilities caused by the experimental probes, make an experimental investigation challenging. At present, most
30 reports discuss the macroscopic properties of the water bridge like its mass, substance and charge transport, its density and temperature gradients and the potential presence of microdomains⁴⁻⁸. The macroscopic stability of the water bridge has been explained in the framework of electrohydrodynamic
35 theory from the balance between the induced polarization forces at the surface, capillary forces, and gravity⁹⁻¹¹. According to these findings, the most important properties necessary for liquid bridge formation are high dielectric permittivity, low electric conductivity and a permanent molecular dipole moment. Thus the
40 phenomenon is not water specific, but can be obtained with any liquid of similar properties like methanol¹² or glycerol⁹.

An interesting question is whether the macroscopic phenomenon of water bridge formation is associated with detectable changes of water on the molecular scale. The
45 molecular-scale properties of the water bridge have been studied with Raman scattering¹³, neutron scattering¹⁴, and dielectric relaxation spectroscopy¹⁵. The results of the neutron scattering experiments indicate the presence of nano bubbles (domains exhibiting lower density) in the water bridge, which could explain

50 some of the observed macroscopic effects. The Raman spectrum of the O-H stretch vibrations of the water bridge is somewhat blue shifted in comparison to the Raman spectrum of bulk liquid water, indicating a slight weakening of the hydrogen bonds. On the other hand, dielectric measurements suggest that the
55 microscopic hydrogen-bond structure is not different from that of bulk liquid water^{9,15}. Unfortunately, molecular dynamics simulations cannot help in elucidating the molecular-scale properties of the water bridge, as the number of water molecules that can be included in these simulations is limited. Molecular
60 dynamics simulations do show effects of electric fields on water clusters, but these calculations concerned electric fields that are ~1000 times higher than needed to form the water bridge^{16,17}.

At present it is an open question whether the water bridge
65 differs from ordinary bulk water on the molecular scale or just represents a macroscopic space charge effect with negligible associated microscopic effects. Here we present a study of the vibrational energy relaxation dynamics of water molecules in the water bridge. The rate of the vibrational energy relaxation is strongly dependent on the direct molecular environment (local
70 hydrogen-bond strength and structure)¹⁸.

Experiment

We measured the vibrational energy relaxation dynamics using polarization-resolved femtosecond mid-infrared pump-probe spectroscopy¹⁹. In the experiment the OH stretch vibration of
75 HOD/D₂O mixture was excited from the vibrational ground state $v=0$ to the first excited state $v=1$ with an intense (~10 μ J) pump pulse. This excitation leads to a bleaching of the fundamental $v=0\rightarrow 1$ transition and an induced $v=1\rightarrow 2$ excited-state absorption. The latter absorption is redshifted by ~250 cm^{-1} due
80 to the anharmonicity of the O-H stretch vibration. The transient changes in absorption were monitored with a much weaker probe pulse. Both pump and probe pulses were centered at 3500 cm^{-1} and had a spectral width of ~350 cm^{-1} . This spectral width is larger than the width of the absorption band of the OH stretch
85 vibration of HDO:D₂O. As a result, spectral diffusion effects are negligible.

We measured the pump-induced frequency-resolved transient

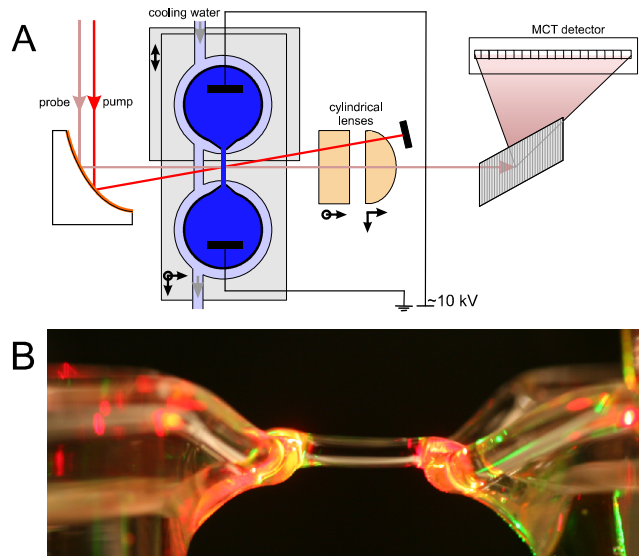


Fig 1. Panel A: Schematic representation of the setup. Black arrows indicate the translation direction of the two beakers and the cylindrical lenses. Panel B shows a picture of the water bridge.

absorption spectra ($\Delta\alpha$) as a function of the time delay between the pump and probe pulses. The pump and probe pulses were focused into the sample with a gold-coated parabolic mirror (see Fig. 1A). After travelling through the sample the probe was recollimated using two cylindrical lenses ($f_1=25$ mm and $f_2=35$ mm) oriented orthogonally with respect to each other. We could thus compensate for the lensing effects resulting from the cylindrical shape of the water bridge. The reference beam (which passed along the sample) was used to correct for shot-to-shot fluctuations of the probe-pulse energy. The probe and reference beams were dispersed with an Oriel monochromator and detected with a 2x32 pixel mercury-cadmium-telluride (MCT) detector array (Infrared Associates).

The polarization of the probe pulses was set to an angle of 45° with respect to the pump pulse polarization. After the sample either the p (parallel to long water bridge axis) or s (parallel to short water bridge axis) probe polarization component was selected using a wire grid polarizer mounted in a motorized rotation stage. The thus obtained transient absorption changes $\Delta\alpha_{\parallel}(t,v)$ and $\Delta\alpha_{\perp}(t,v)$ were used to construct the so-called isotropic signal $\Delta\alpha_{\text{iso}}(t,v)=1/3[\Delta\alpha_{\parallel}(t,v)+2\Delta\alpha_{\perp}(t,v)]$.

The delay time-dependent isotropic pump-probe signal $\Delta\alpha_{\text{iso}}(t,v)$ is not sensitive to the depolarization of the excitation and directly reflects the vibrational energy relaxation.

The water bridge sample was prepared as reported previously.^{5,14} Briefly, two 100 mL glass beakers were filled with a dilute solution of HDO in D_2O (Cambridge Isotope Laboratories DLM-6, D-99.96%, conductivity ~ 1.4 $\mu\text{S}/\text{cm}$). Rectangular, platinum electrodes were placed in each beaker. One of the electrodes was grounded, the other one had a potential between 6 and 13 kV applied with a FUG high voltage power supply (HCP 140-20000, 6 mA, 20 kV). The current varied between 40 μA and 200 μA , depending on the water bridge length and thickness. The beakers were kept at a constant temperature ($20^\circ \pm 2^\circ\text{C}$) in order to minimize thermal effects in the sample and to improve the bridge stability. The beakers were placed on translation stages allowing for spatial adjustment of the width and length of the water bridge (Fig. 1A).

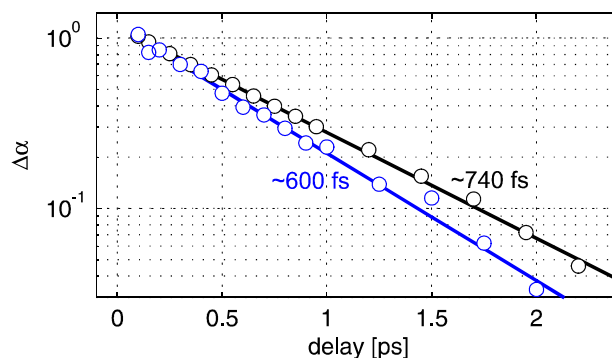


Fig 2. Normalized delay traces for the water bridge (blue circles) and for the reference bulk sample (black circles). The traces are measured at a probe frequency of 3500 cm^{-1} , where the heating effect is negligible. The lines are guide to the eyes resulting from monoexponential fit.

We tuned the parameters of the water bridge in order to obtain the best compromise between bridge stability (which is achieved with a thick bridge) and a not too high optical density (which is attained for a thin bridge). We obtained an optimal result with a voltage of approximately 9 kV (1.5 kV/cm) and a current of about 60 μA , and the bridge having a length of 1.0–1.5 cm and a thickness of about 2–3 mm.

We also performed reference experiments on a sample of bulk HDO: D_2O . The sample cell used in these reference experiments was formed by two 2 mm CaF_2 windows separated by a 1.5 mm teflon spacer. The cell was filled with a sample taken from the HDO: D_2O liquid that was also used to form the water bridge. From the linear absorption spectrum it followed that this sample was a dilute solution of $\sim 0.5\%$ HDO in D_2O . The experiments on the water bridge and the reference sample were repeated many times with excellent reproducibility.

Results and discussion

In Figure 2 we show pump-probe signals as a function of delay for the water bridge and the reference bulk sample. For both samples, the signal was normalized to the value at 0.2 ps delay. The pump excitation of the $\nu=1$ state of the OH stretch vibration resulted in a bleaching signal for the weak probe pulse. This bleaching is partly due to the depletion of the ground state, thereby reducing the absorption from the ground state ($\nu=0 \rightarrow 1$), and partly due to stimulated emission out of the excited state back to the ground state ($\nu=1 \rightarrow 0$). The $\nu=1$ state relaxes back to the ground state ($\nu=0$), thus leading to a decay of the bleaching signal. Both traces shown in Figure 2 were obtained by spectrally averaging over a frequency interval of 30 cm^{-1} centered around 3500 cm^{-1} . At this frequency the final thermal effect of the excitation is minimal.

The results show that the vibrational relaxation is significantly faster for the water bridge than for bulk HDO: D_2O . A single exponential fit to the data yields vibrational relaxation time constants T_1 for the HDO: D_2O water bridge and for bulk HDO: D_2O of 600 ± 30 fs and 740 ± 30 fs, respectively. The vibrational lifetime of the water bridge is thus significantly shorter than that of ordinary bulk liquid water. The shorter lifetime of the water bridge is observed at different positions in the bridge. Hence, there is no gradient of this lifetime. The relaxation time found for bulk HDO: D_2O is in excellent agreement with the results of previous studies^{18,20}.

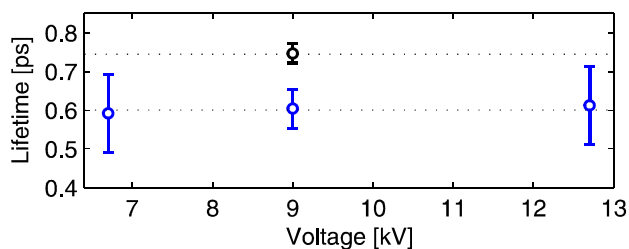


Fig 3. OH stretch vibrational lifetime determined from the delay-time curves measured for the water bridge for three different applied potentials (blue) and for the reference sample (black). The values were obtained by averaging the lifetime values over many measurements (10 for the water bridge and 15 for the reference). The larger error bars for the lifetimes at 6.7 kV (1.1 kV/cm) and 12.7 kV (2.1 kV/cm) originate from the smaller number of measurements performed at these voltages (3 and 2 respectively). The reference sample was not exposed to any potential (position of the data point is purely for comparison).

To study whether the applied potential has an effect on the vibrational lifetime of the HDO molecules in the water bridge, we also performed experiments using potentials of 6.7 kV (1.1 kV/cm) and 12.7 kV (2.1 kV/cm). As depicted in Figure 3 no significant dependence of the lifetime on the applied potential was observed. At all potentials we observed a shortened vibrational lifetime of ~ 600 fs. However, it should be noted that at each potential we had to adjust the length of the water bridge to keep it stable. Hence, the local electric fields in the water bridge may in fact not be very different for these (externally) applied potentials.

We performed experiments both with the pump beam polarized along the long axis of the water bridge (p-polarized) and perpendicular to the long axis of the water bridge (s-polarized). For both configurations we observed a vibrational lifetime of 600 ± 30 fs. Hence, the vibrational relaxation does not depend on the orientation of the excited OH vibrations in the water bridge.

In order to exclude the possibility of artifacts and to find the origin of the acceleration of the vibrational relaxation rate for the water bridge, we performed additional test experiments on the reference sample. In the first experiment we varied the optical density. In the second experiment we applied an electric field (2 kV/cm) to the reference sample by either placing the sample in between the two electrodes (with no direct contact between water and the electrodes) or by sliding the two electrodes in between the windows, thus exposing the water film to the electric field directly. In all these studies we obtained the same vibrational lifetime for the reference sample of 740 ± 30 fs. The latter result shows that the shortening of the vibrational lifetime is not directly due to the presence of the electric field. This result is in line with the lack of dependence of the vibrational lifetime of the bridge on the pump polarization. Water molecules oriented parallel and perpendicular to the electric field lines show the same shortened relaxation time, thus confirming the notion that the electric field itself is not responsible for the shortening of the lifetime.

One may think that the shorter vibrational lifetime of the water bridge could be the result of a local heating effect, as the current running through the water bridge leads to a local rise in temperature⁴. For most substances, an increase in temperature leads to an acceleration of vibrational energy transfer processes. However, one of the anomalous properties of water is that its vibrational lifetime *increases* with rising temperature¹⁸. This anomalous behavior can be explained by the blueshift of the OH

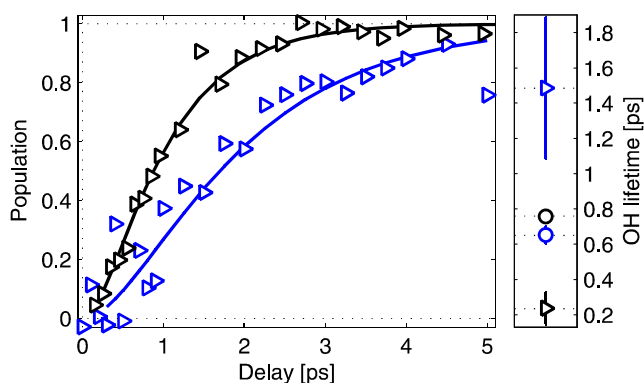


Fig 4. Thermalization dynamics of the water bridge (in blue) and the bulk sample (black) following the relaxation of the OH stretch mode. Right panel shows the extracted lifetimes for the excited (circles) and intermediate states (triangles).

stretch vibrational spectrum with temperature. Due to this blueshift, the coupling to lower-frequency accepting modes decreases, and thus the T_1 lifetime increases. In a Raman study of the water bridge a small blueshift of the OH stretch vibration spectrum was observed¹³, which is thus also consistent with a heating effect in the water bridge. Hence, based on the temperature effect, a small increase of the vibrational lifetime of the water bridge would have been expected, which makes the observed shortening of this lifetime all the more surprising. For a bulk liquid HDO:D₂O sample the observed lifetime of $\sim 600 \pm 30$ fs would correspond to a temperature below 0°C ¹⁸. Of course, the water bridge in our study is not supercooled but had a temperature of $25 \pm 2^\circ\text{C}$ (measured with a thermographic camera calibrated to the emissivity of water⁵), thus slightly higher than the water in the beakers.

We also analyzed the equilibration (thermalization) of the vibrational energy following the relaxation of the OH stretch vibration. It has been observed before that the vibrational relaxation of the OH stretch vibration of bulk HDO:D₂O and of the OD stretch vibration of HDO:H₂O does not directly lead to a thermal equilibration of the vibrational energy²¹. The thermalization is delayed because the state(s) that get excited by the relaxation of the OH/OD stretch vibration do not represent a thermal energy distribution, and because it takes some time before the structure (coordinates) of the hydrogen-bond network reaches the new equilibrium configuration that corresponds to the higher energy content of the low-frequency modes. In the present experiments we also observed that the rise of the thermally equilibrated absorption spectrum was delayed with respect to the decay of the excited state spectrum. To quantify this delay we described the data with a model that involves three states: the excited state, an intermediate state and a final heated state. The exact character of the intermediate state in the relaxation process is not clear, but likely involves the simultaneous excitation of many modes (i.e bend mode, librations, H-bond stretch).

Figure 4 shows the result of a global fit to the data at all probe frequencies. The fitting results are represented by solid lines. The fit to the three-level model yields a similar time constant for the excited state relaxation of the OH stretch vibration as was obtained from the analysis of the data in the frequency regions where the heating effect on the signal is negligible. We found $T_{1\text{WB}} = 630 \pm 50$ fs and $T_{1\text{Bulk}} = 740 \pm 40$ fs.

Interestingly, we found that the rise of the heated end level is much slower for the water bridge ($T_{\text{eqWB}}=1.5\pm 0.4$ ps) than for the bulk sample ($T_{\text{eqBulk}}=250\pm 90$ fs). The right panel in figure 4 presents the extracted relaxation time constants. The error bars reflect the spread of the lifetimes over all the analyzed data sets (15 for the water bridge – including data at higher and lower potential and s excitation polarization, and 15 for the reference sample).

Thus the formation of the water bridge has an even stronger effect on the thermalization dynamics than on the energy relaxation of the OH stretch vibration. It is also interesting to note that the effects are opposite: the vibrational relaxation of the OH vibration is accelerated, whereas the equilibration of the system is slowed down. Both changes in vibrational relaxation dynamics hint at a different structural arrangement of water molecules in the water bridge compared to bulk liquid water.

A structural rearrangement responsible for the observations could be formed by a partial collapse of the tetrahedral network of water. Such a collapse is supported by 2D neutron and Raman scattering studies that found evidence that in the water bridge the number of hydrogen bonds per water molecule is reduced and that the water molecules are partially aligned^{13, 22}. A partial collapse of the hydrogen bond network will reduce the connectivity of the water molecules, which can thus explain the slowing down of the thermalization of the energy, as this process requires the equilibration of the energy over many water molecules.

A partial collapse of the network will also affect the modes that accept the energy of the excited OH stretch vibration. These modes are the HDO bending mode (~ 1450 cm⁻¹), the librations (~ 800 cm⁻¹), the hydrogen-bond stretch vibrations (~ 200 cm⁻¹) and the hydrogen-bond bend vibrations (~ 50 cm⁻¹). Especially the lower-energy accepting modes are quite susceptible to structural rearrangements, and changes in their frequency and coupling to the OH stretch vibration could explain the observed acceleration of the vibrational energy relaxation.

Conclusions

In conclusion, we studied the energy relaxation of the OH stretch vibration of HDO molecules contained in an HDO:D₂O water bridge. We found that the vibrational relaxation is significantly faster ($\sim 630\pm 50$ fs), and that the subsequent thermalization dynamics are significantly slower (1.5 ± 0.4 ps) than in bulk HDO:D₂O (740 ± 40 fs, 250 ± 90 fs respectively). These effects are not induced directly by the electric field that is needed to form the water bridge. Instead these observations appear to result from a different molecular-scale structure of water in the water bridge.

Acknowledgements

The work is part of the research program of the Foundation for Fundamental Research on Matter (FOM) which is financially supported by the Dutch organization for Scientific Research (NWO). Moreover, this work was performed in the TTIW-cooperation framework of Wetsus, Centre of Excellence for Sustainable Water Technology. The financial support of the Applied Water Physics Theme of Wetsus is thankfully acknowledged.

Notes and references

^a FOM Institute for Atomic and Molecular Physics – AMOLF, Science Park 104, 1098 XG Amsterdam, The Netherlands;

⁶⁰ E-mail: piatkowski@amolf.nl

^b Wetsus—Centre of Excellence for Sustainable Water Technology, Agora 1, 8900 CC Leeuwarden, The Netherlands

1. W. G. Armstrong, *The Newcastle Literary and Philosophical Society, The Electrical Engineer*, 1893, 154-155.
2. F. Mugele and J. C. Baret, *J. Phys. Condens. Matter*, 2005, **17**, R705.
3. I. Sumoto, *Oyo Butsuri*, 1956, **25**, 264.
4. E. Del Giudice, E. C. Fuchs and G. Vitiello, *Water (Seattle)*, 2010, **2**, 69-82.
5. J. Woisetschlager, K. Gatterer and E. C. Fuchs, *Exp. Fluids*, 2010, **48**, 121-131.
6. H. Nishiumi and F. Honda, *Res. Lett. Phys. Chem.*, 2009, **ID371650**.
7. M. a. G. Eisenhut, X., A. H. Paulitsch-Fuchs and E. C. Fuchs, *Cent. Eur. J. Chem.*, 2011, **9**, 391-403.
8. E. C. Fuchs, L. L. F. Agostinho, M. Eisenhut and J. Woisetschlager, *J. Proc. SPIE*, 2010, **7376**, 73761E.
9. A. G. Marin and D. Lohse, *Phys. Fluids*, 2010, **22**, 122104.
10. A. Widom, J. Swain, J. Silverberg, S. Sivasubramanian and Y. N. Srivastava, *Phys. Rev. E*, 2009, **80**, 016301.
11. A. A. Aerov, arXiv:1012.1592v1., 2010.
12. E. C. Fuchs, *MDPI Water*, 2010, **2** 381-410.
13. R. C. Pontiero, M. Pochylski, F. Aliotta, C. Vasi, M. E. Fontanella and F. Saija, *J. Phys. D: Appl. Phys.*, 2010, **43**, 175405.
14. E. C. Fuchs, B. Bitschnau, J. Woisetschlager, E. Maier, B. Beuneu and J. Teixeira, *J. Phys. D: Appl. Phys.*, 2009, **42**, 065502.
15. F. Saija, F. Aliotta, M. E. Fontanella, M. Pochylski, G. Salvato, C. Vasi and R. C. Pontiero, *J. Chem. Phys.*, 2010, **133**, 081104.
16. Y. C. Choi, C. Pak and K. S. Kim, *J. Chem. Phys.*, 2006, **124**, 094308.
17. D. Rai, A. D. Kulkarni, S. P. Gejji and R. K. Pathak, *J. Chem. Phys.*, 2008, **128**, 034310.
18. S. Woutersen, U. Emmerichs, H.-K. Nienhuys and H. J. Bakker, *Phys. Rev. Lett.*, 1998, **81**, 1106-1109.
19. L. Piatkowski and H. J. Bakker, *J. Phys. Chem. A*, 2010, **114**, 11462-11470.
20. C. J. Fecko, J. J. Loparo, S. T. Roberts and A. Tokmakoff, *J. Chem. Phys.*, 2005, **122**, 054506.
21. T. Steinel, J. B. Asbury, S. A. Corcelli, C. P. Lawrence, J. L. Skinner and M. D. Fayer, *Chem. Phys. Lett.*, 2004, **386**, 295 - 300.
22. E. C. Fuchs, P. Baroni, B. Bitschnau and L. Noirez, *J. Phys. D: Appl. Phys.*, 2010, **43**, 105502.